Drought assessment

a) Development of a drought monitoring and prediction system and agricultural impact assessment

(1) Northeastern Brazil

ICHARM developed a DIAS drought monitoring and prediction system for Northeastern Brazil, based on the Coupled Land and Vegetation Data Assimilation System (CLVDAS) (Figure 1). We also developed a method to estimate cashew-nut and feijão-bean yields for the period from 2003 to 2013 using leaf area index (LAI) outputs produced by the developed system for Ceará State, an agriculturally active region. Using these developments, cashew-nut and feijão-bean yields were estimated for the period from 2014 to 2017. The results showed good agreement with agricultural statistical data, with RMSE values below 0.06 t and bias values of 0.03 t.

To improve the spatial resolution of LAI outputs from CLVDAS, we used the WEB-DHM-Veg model, a coupled model integrating the WEB-DHM model and the dynamic vegetation model. We then developed a method to estimate feijão-bean yields using the higher resolution LAI for 16 districts of the Banabuiú River basin, a particularly agriculturally active area in Ceará State, and estimated feijão-bean yields for the period from 2014 to 2017, when a severe drought occurred (Figure 2). In this estimation as well, the results showed good agreement with agricultural statistical data, with relative errors below 12%, in most of the 16 districts (Figure 3).

Focusing on the mean yields from 2014 to 2017, we found that relative errors were larger in the eastern part of the Banabuiú River basin, which corresponds to the irrigated area. Therefore, we conducted test calculations of the actual amount of irrigation water supplied in 2014 and 2015, and found that irrigation water was supplied at approximately 4.5 mm/sec in 2014 and approximately 3.5 mm/sec in 2015.

In addition, we predicted feijão-bean yields for 2018 using hindcast LAI data of the same year, which were produced by the DIAS drought monitoring and prediction system. The predicted yields indicated that this approach can achieve a level of accuracy comparable to that of real-time monitoring (Figure 4). Through this verification process, we confirmed that our drought monitoring and prediction system can be instrumental not only for monitoring and forecasting ecohydrological variables, but also for assessing agricultural impacts and supporting agricultural activities.

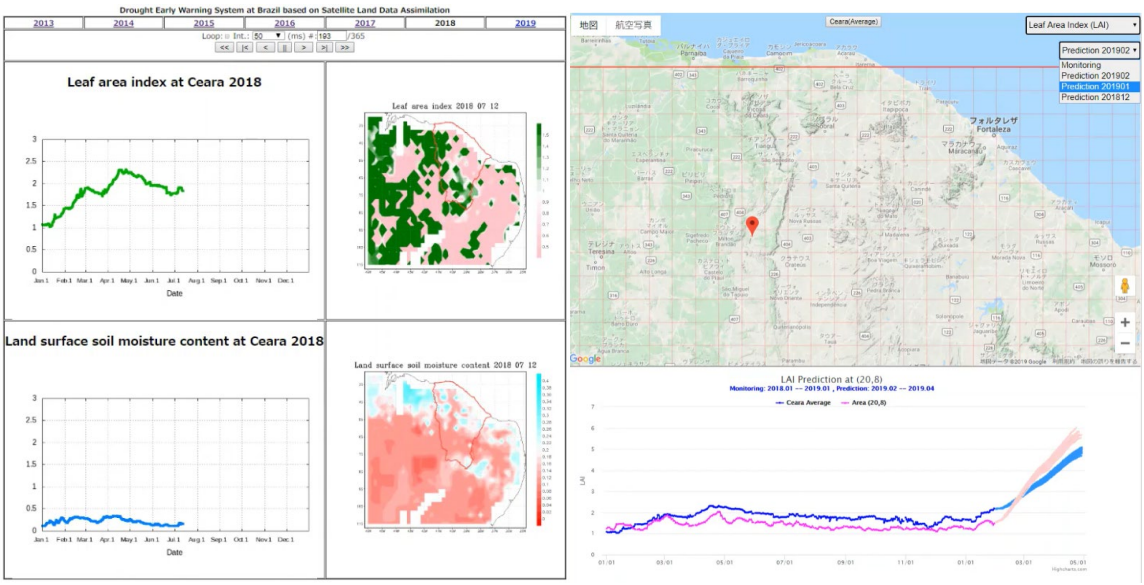


Figure 1 DIAS drought monitoring and prediction system for Northeastern Brazil

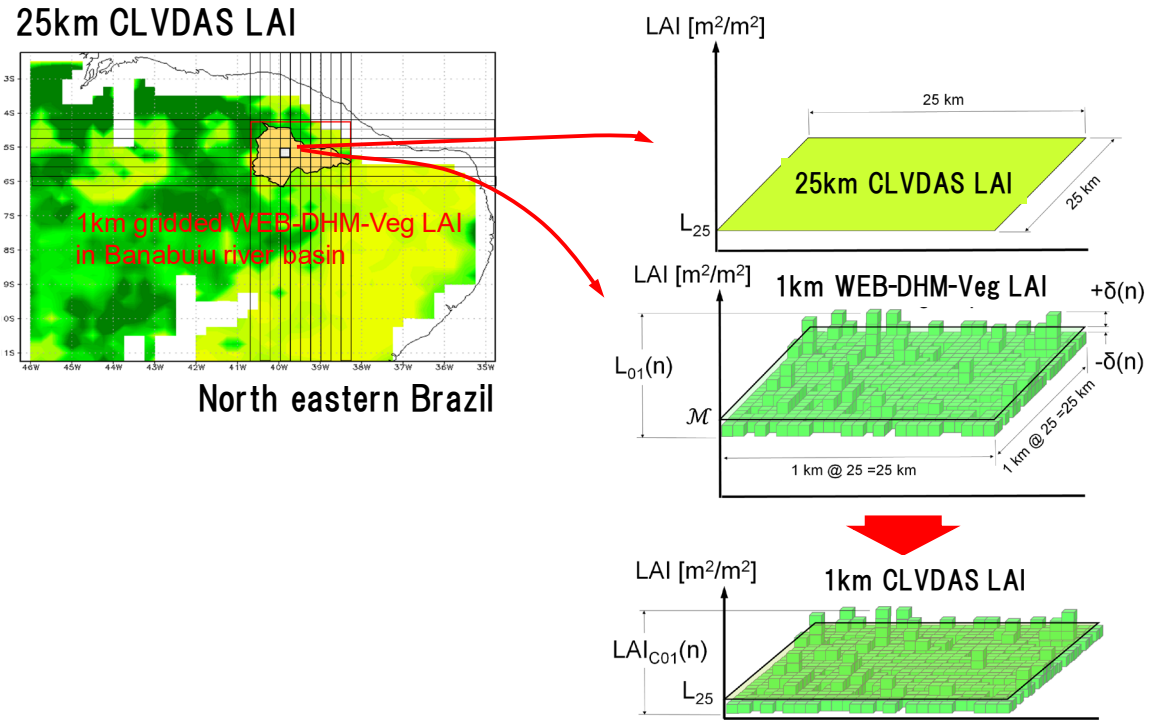


Figure 2 CLVDAS LAI High-Resolution Enhancement Method

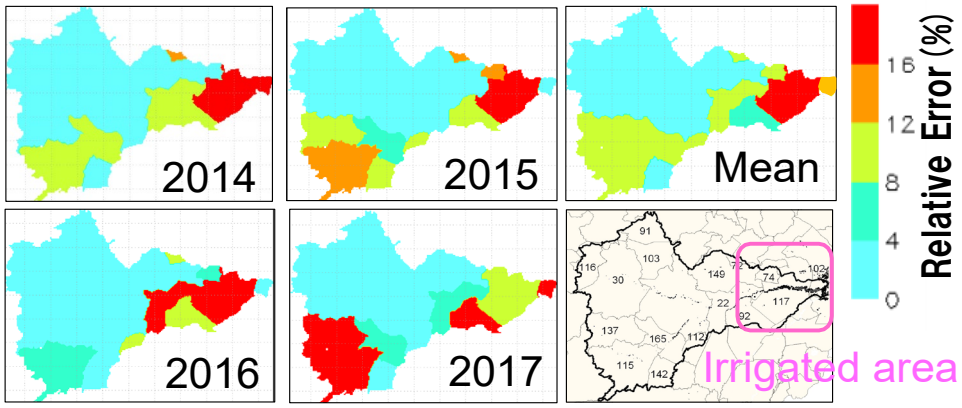


Figure 3 Relative error (%) between estimated and statistical yields of feijão beans in 16 districts of the Banabuiú River basin in Ceará state.

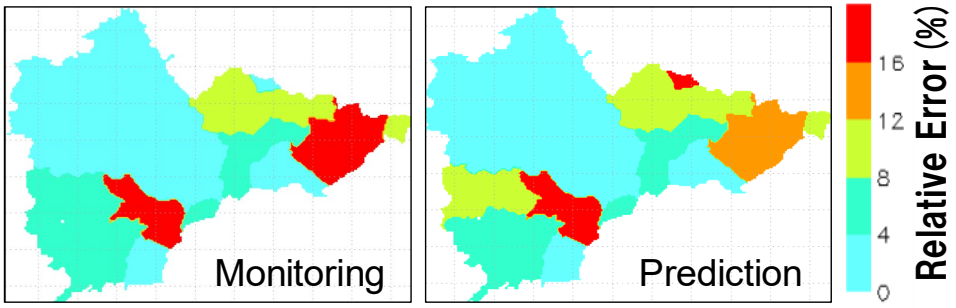


Figure 4 Relative error (%) between 2018 hindcast predicted yield and statistical yield of feijão beans in 16 districts of the Banabuiú River basin in Ceará state: (Left) Monitoring, (Right) Handcast prediction

(2) Republic of Ghana

ICHARM developed a DIAS drought monitoring and prediction system for Ghana based on the CLVDAS system (Figure 5). Furthermore, we developed a method to estimate corn yields using vegetation-water-content outputs produced by the developed system for 13 districts of Brong-Ahafo State, an agriculturally active region. Figure 6 shows the estimated corn yields for these districts. In the ASUNAFO and ASUTIFI districts (blue frame) and the NKORANZA and KINTAMPO districts (orange frame), corn yields are high because vegetation water content is high in both wet and dry years. In contrast, in the WENCHI and TECHIMAN districts (pink frame), corn yields are low because vegetation water content is low in the dry year due to drought impact, while corn yields are high because vegetation water content is high in the wet year. These results indicate that vegetation water content varies among districts due to the spatial distribution of root-zone-soil moisture content, and that corn yields correspondingly vary with this distribution.

Furthermore, we estimated corn yields using vegetation-water-content monitoring outputs for the period 2004 to 2022 and found good agreement with agricultural statistical data, with an RMSE of 2.1 t/ha. In addition, when the 2018 corn yield was predicted using hindcast vegetation-water-content data in 2018, the difference from the agricultural statistical data was only 0.2 t/ha. From these cases, we confirmed that drought

assessment and crop-yield estimation and prediction in each district are feasible when district-scale agricultural statistical data are available.

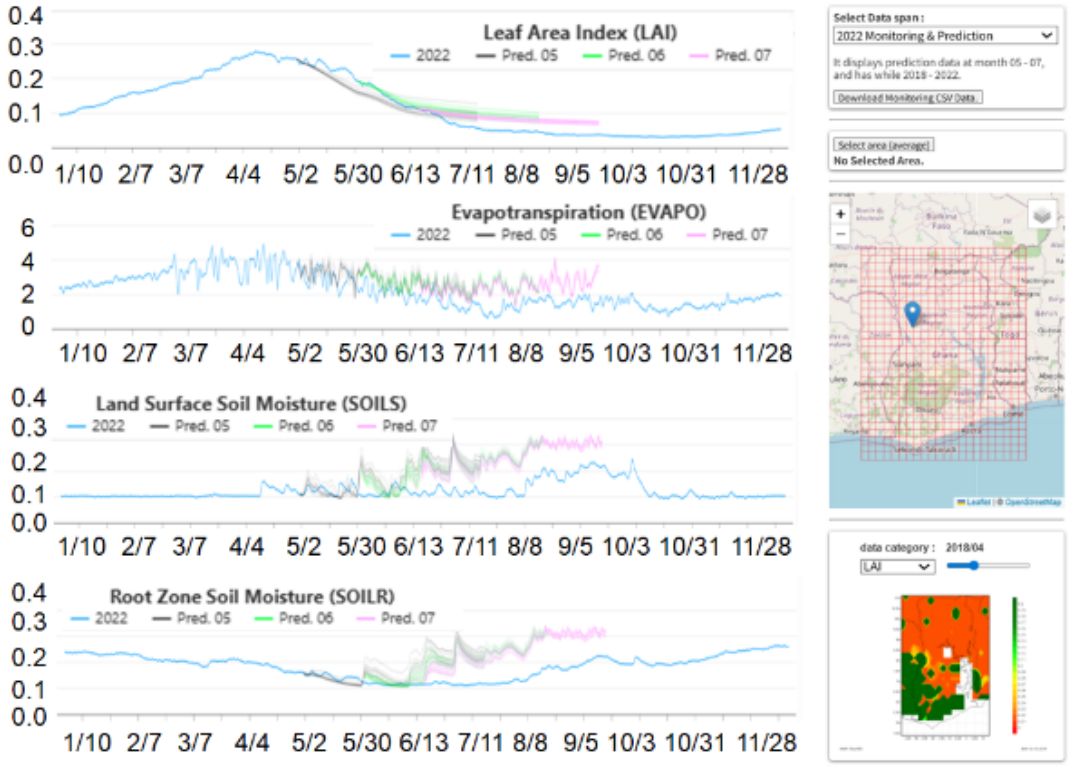


Figure 5 DIAS drought monitoring and prediction system for Ghana

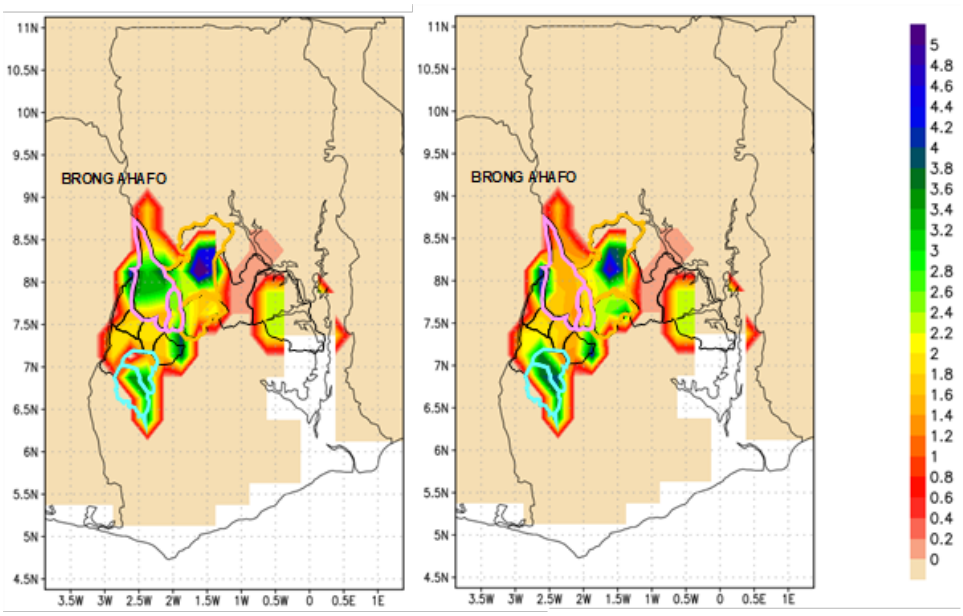


Figure 6 Spatial distribution of estimated corn yields in Brong-Ahafo province: Left figure shows humid years, right figure shows dry years. Blue box represents the ASUNAFO/ASUTIFI district, orange box represents the NKORANZA/KINTAMPO district, and pink box represents the WENCHI/TECHIMAN district.

(3) Republic of South Sudan

ICHARM developed a drought monitoring system based on CLVDAS and conducted long-term simulations for the period from 2004 to 2023. We also developed a method for estimating corn and sorghum yields from vegetation-water-content outputs produced by the developed system. The results showed that corn and sorghum yields remain high in Upper Nile, Pibor, and Eastern States, as well as parts of Central Equatoria State, even during drought years because soil moisture is consistently abundant (Figure 7a); therefore, the irrigation effect is low (Figure 7b). In other areas, yields are low because soil moisture is consistently low (Figure 7a), resulting in a high irrigation effect (Figure 7b). Yields were estimated to be high in 2021 (Figure 8b,c). However, they came closer to FAO statistical yields (Figure 8b, c) after setting the estimated yields in harvest areas overlapping with flood inundated zones (Figure 8a) to zero. This case demonstrates that agricultural drought can be assessed at the farm level when information on harvest areas and locations is available. It also suggests that drought-related agricultural damage should be evaluated seamlessly together with flood damage.

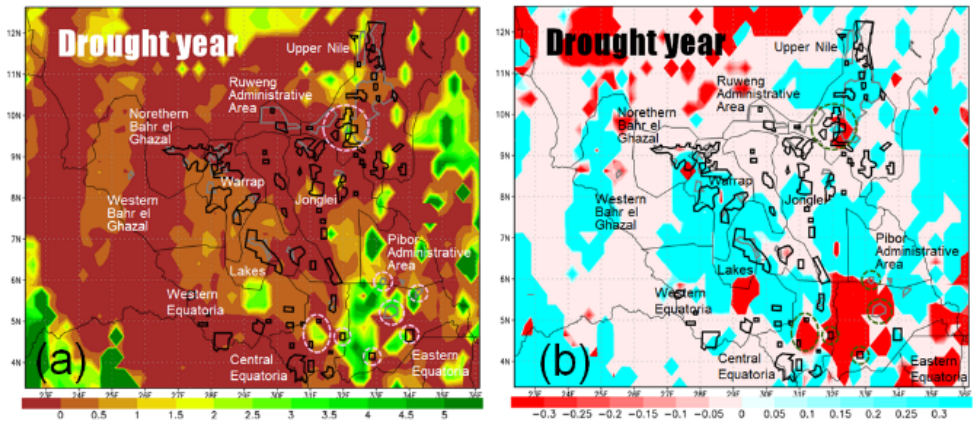


Figure 7 (a) Estimated yield (x10⁹ t) and (b) Irrigation effectiveness: Corn (gray) and Sorghum (black)

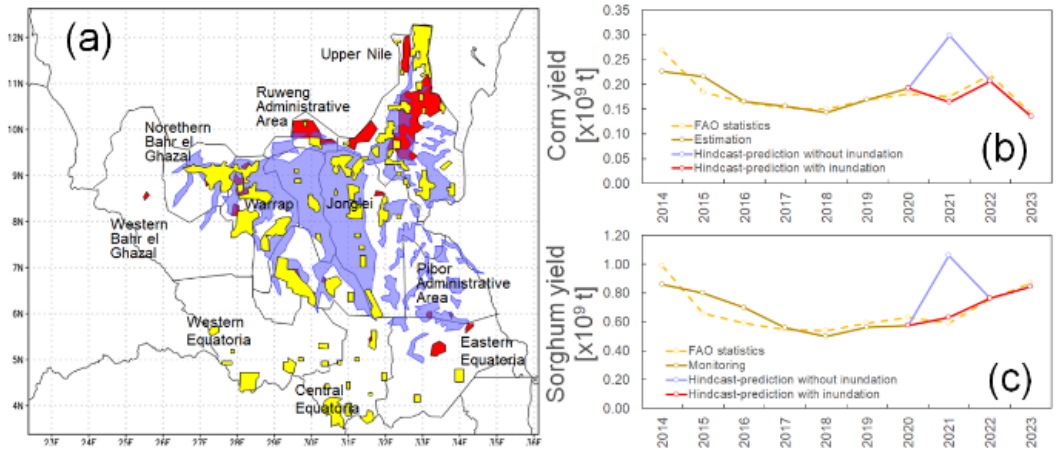


Figure 8 (a) Corn (red), sorghum (yellow), and 2021 flood inundation area (blue); (b)(c) Estimated corn and sorghum yields: (solid brown line) FAO statistical yield, (dashed yellow line) 2014-20 estimated yield, (solid blue line) 2021-23 estimated yield without considering the 2018 flood, (solid red line) 2021-23 estimated yield considering the 2018 flood.

b) Agricultural drought assessment using CLVDAS over the Intertropical Convergence Zone (ITCZ) and the subtropical high region

ICHARM assessed agricultural drought trends for the period from 2004 to 2017 using CLVDAS for six regions (West Africa, Malawi, Northeast Brazil, Jordan, India, and Guatemala) located in the Intertropical Convergence Zone (ITCZ) and the subtropical high region (Figure 9). The results showed good agreement in the normalized index (Z-score) between estimated vegetation water content and corn statistical yield. The analysis also indicated that droughts during 2004-2017 could be classified into three types: Type A, occurring in the late period, Type B, occurring in the early period, and Type C, occurring irregularly (Figure 10).

We also analyzed atmospheric boundary layer conditions and found that, in Type A, variations in the extent of updrafts in the ITCZ between wet and drought years affect land-surface dryness. In Type B, land-surface dryness is affected by the strength of downdrafts caused by the Hadley circulation. In Type C, drought years occur irregularly due to the combined influence of changes in ITCZ updraft extent (Type A) and the strength of Hadley-circulation downdrafts (Type B) (Figure 11).

In addition, we investigated the relationship between drought trends, atmospheric circulation phenomena, and external factors. The results suggested that droughts were associated with severe El Niño events in Northeastern Brazil, Guatemala, West Africa, and India, and with the negative Indian Ocean Dipole mode (IOD) in Marawi (Figure 12a). We also identified locust plague as an external factor causing agricultural damage in West Africa and Jordan (Figure 12b,c,d).

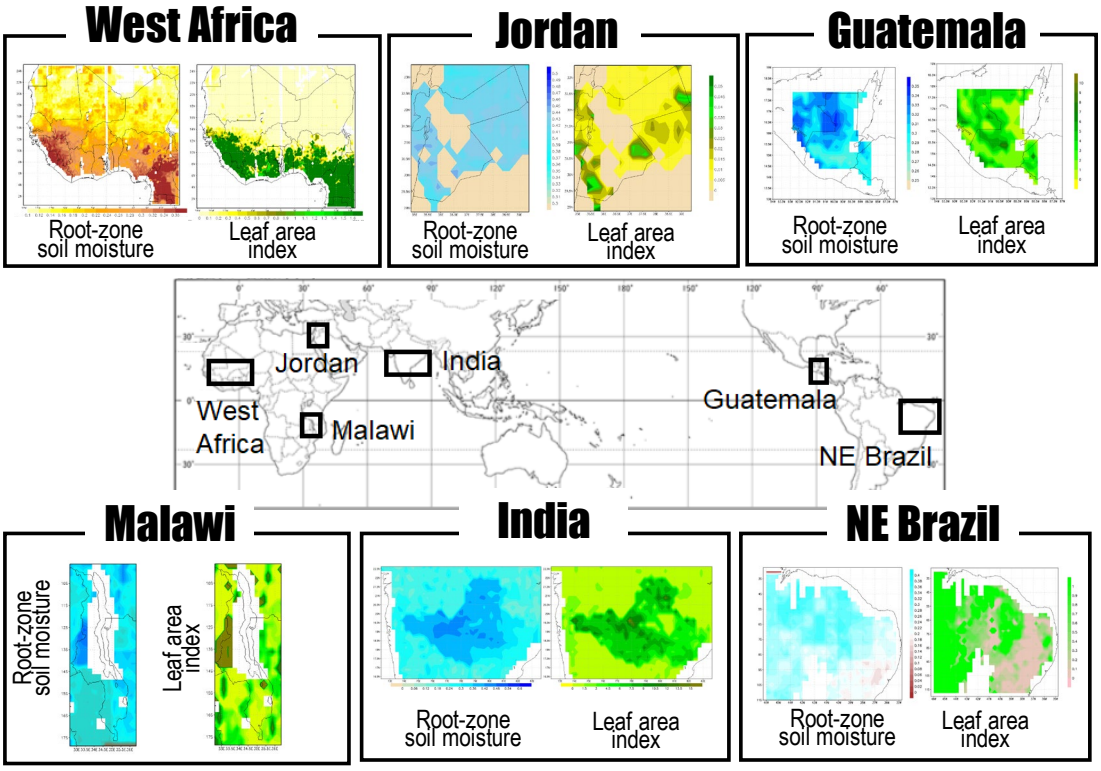


Figure 9 Spatial distribution of ecohydrological variables for six regions (West Africa, Malawi, Northeast Brazil, Jordan, India, and Guatemala) in the intertropical convergence zone (ITCZ) and the subtropical high region.

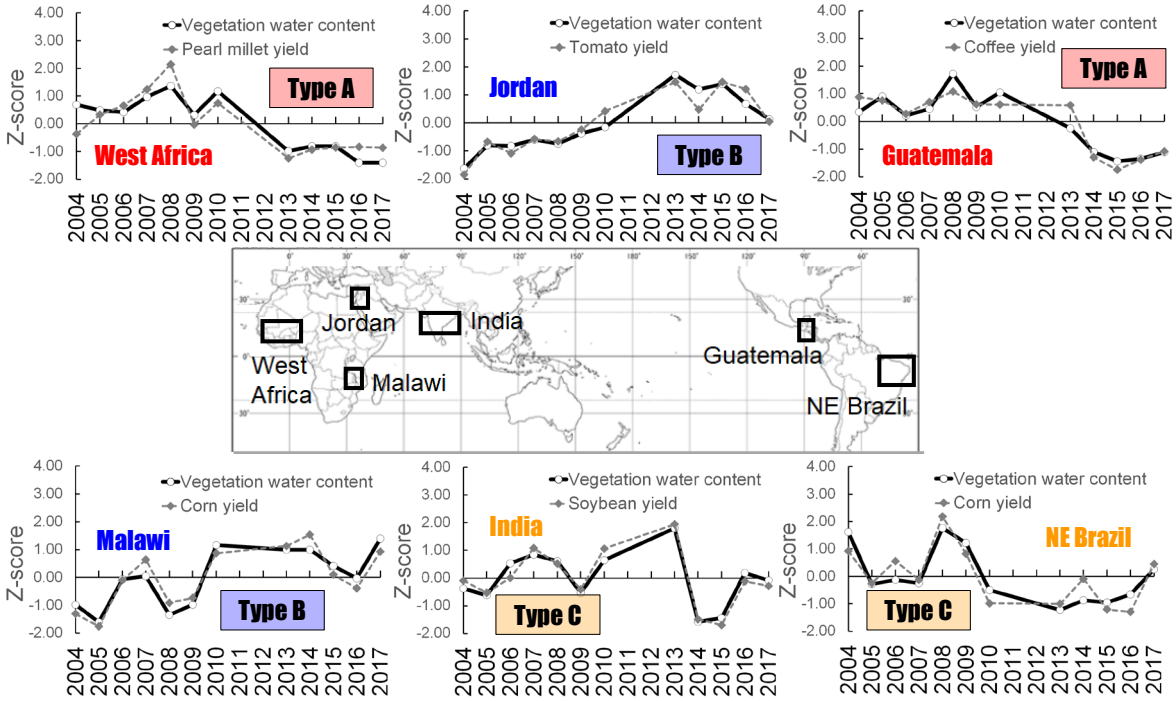


Figure 10 Variation of drought trends for six regions in the intertropical convergence zone (ITCZ) and the subtropical high region: the normalized index (Z-score) of estimated vegetation water content (solid line) and corn statistical yield (dashed line) and classification of drought trends (Type A, B, C)

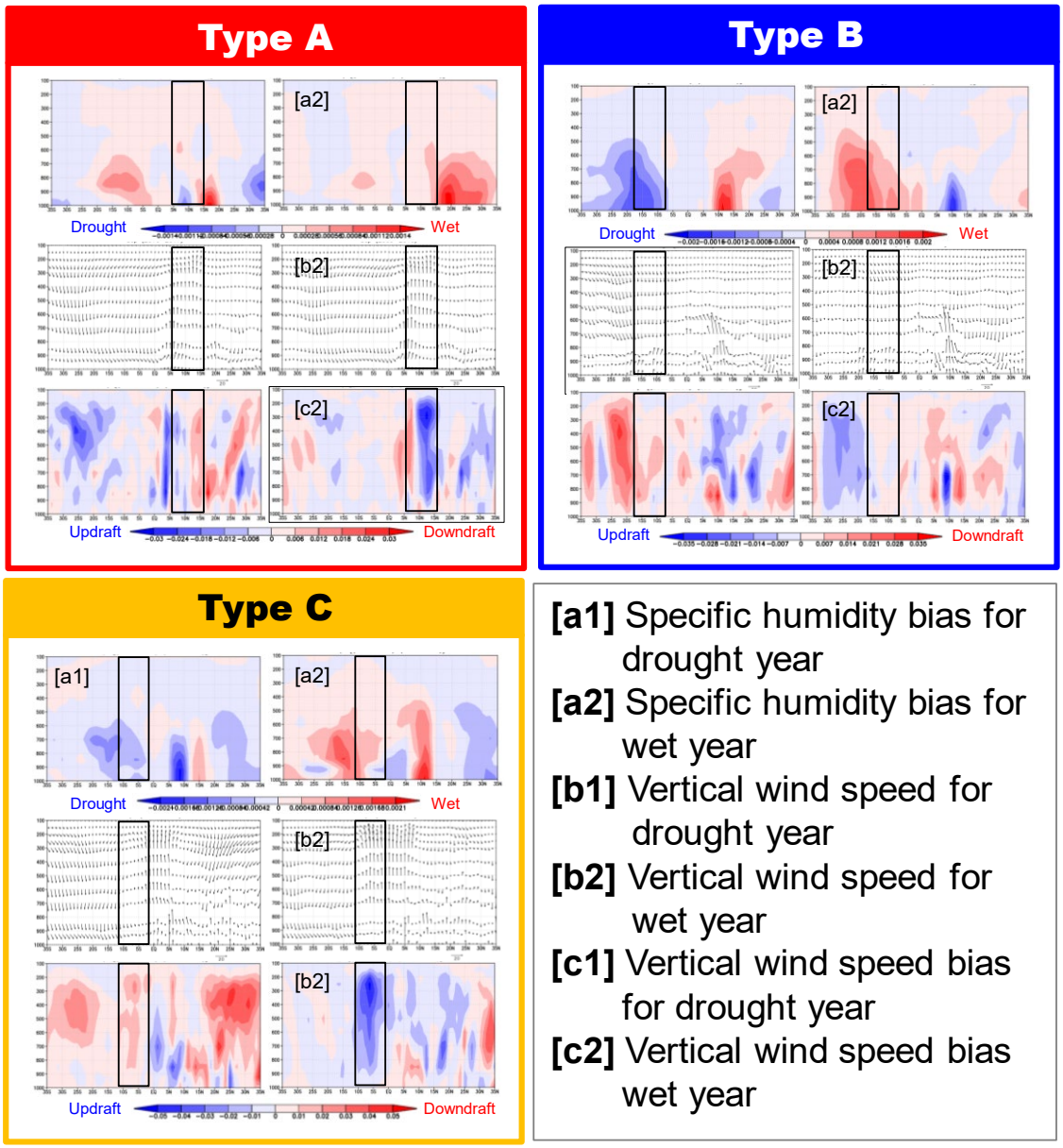


Figure 11 Three types of drought (A, B, C)

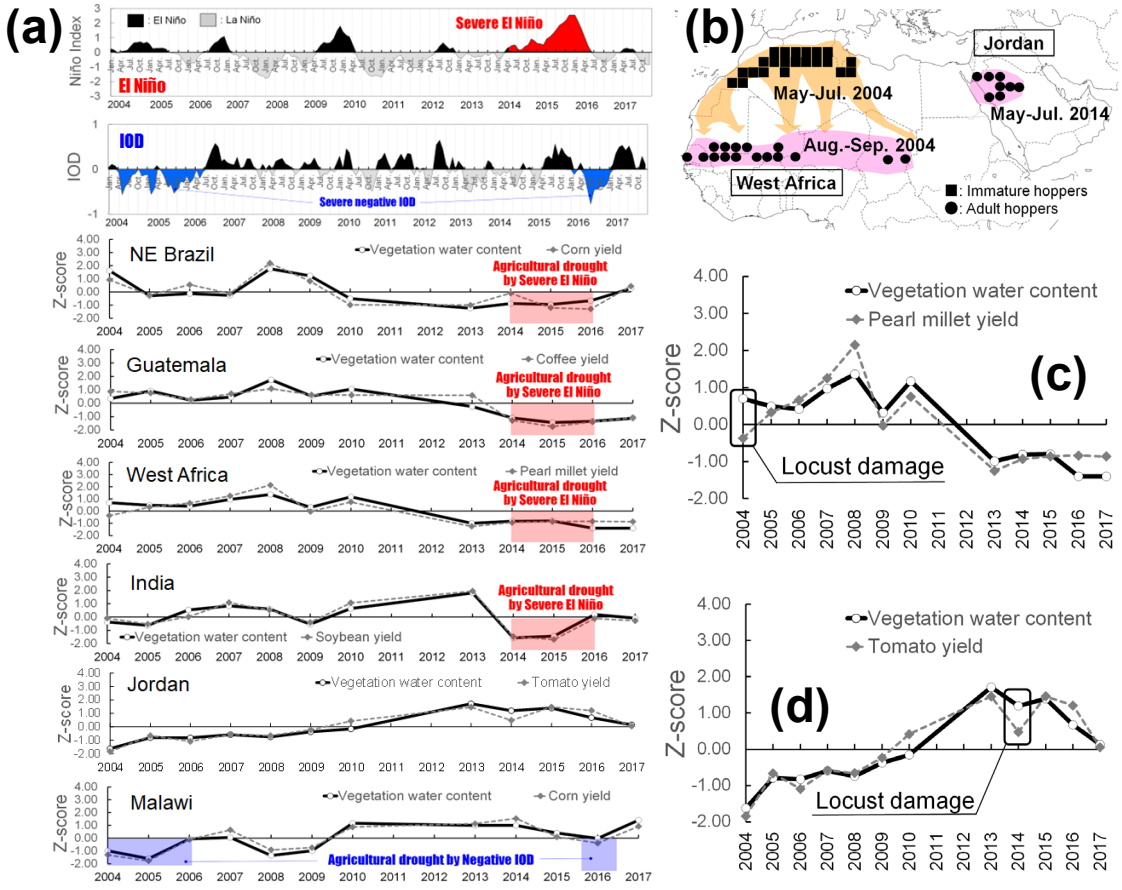


Figure 12 Relationship between drought trends and atmospheric circulation phenomena(a), occurrence information of locust plague as an external factor (b), relationship between locust plague and agricultural products damage (West Africa (c) and Jordan (d))